

## 8. DIRECTIONAL PROPERTIES OF *P*-WAVE VELOCITIES AND ACOUSTIC ANISOTROPY IN DIFFERENT STRUCTURAL DOMAINS OF THE NORTHERN BARBADOS RIDGE ACCRETIONARY COMPLEX<sup>1</sup>

W. Brückmann,<sup>2</sup> K. Moran,<sup>3</sup> and B.A. Housen<sup>4</sup>

### ABSTRACT

Ocean Drilling Program (ODP) Leg 156 revisited the northern Barbados Ridge, where the previous Deep Sea Drilling Program Leg 78A and ODP Leg 110 studied the frontal part of this accretionary prism. Drilling and logging-while-drilling at Sites 947, 948, and 949 successfully identified major thrust faults and the décollement, which was the target of several downhole experiments. Two of the eight holes drilled were equipped with borehole observatories that will monitor temperature, pressure, and fluid flow over the next years. Coring at Hole 948C recovered 180 m of sediment, centered around the décollement, which was positively identified based on structural information. The aim of this study is the evaluation of the possible correlation of preferred orientation of acoustic properties and the direction of maximum compressive strain in the frontal part of the accretionary prism. For this purpose, shipboard *P*-wave velocities from Holes 948C and 949B were reoriented. This information was then used to compare the directional properties of accreted and subducted sediments. In Hole 948C, lowest transverse velocities ( $T_{\min}$ ) were observed to be consistently oriented perpendicular to the maximum horizontal compressive stress, believed to be parallel to the convergence vector. In the underthrust domain of Hole 948C, several preferred orientations for  $T_{\min}$  were detected, but no correlation with the geotectonic reference frame could be identified. Acoustic anisotropy does not show a comparable pattern in Hole 948C. It is concluded that the observed directional dependence of *P*-wave velocity in the accreted sediment domain in Hole 948B is the result of moderate to steeply inclined bedding, although this conclusion can not adequately be tested due to the lack of corrected structural data.

### INTRODUCTION

#### Leg 156 Objectives and Results

The objective of Ocean Drilling Program (ODP) Leg 156 was the experimental evaluation of the temporal and spatial scale of effects, rates, and episodicity of fluid flow in the frontal part of an accretionary complex (Shipboard Scientific Party, 1995a). This task could be accomplished in the northern Barbados Ridge accretionary complex, which had been extensively studied during previous Deep Sea Drilling Project (DSDP) Leg 78A (Biju-Duval, Moore, et al., 1984) and ODP Leg 110 (Moore, Mascle, et al., 1990). From these previous cruises, the stratigraphy, structure, and sedimentology of this accretionary complex, forming at the leading edge of the Caribbean Plate (Fig. 1), are well known (Moore et al., 1988). During Leg 156, eight holes were drilled at Sites 947, 948, and 949. Coring during Leg 156 was minimized, as it was only required to define the exact position of the décollement zone, the target interval for most downhole experiments and long-term observations. Employing an array of new experimental tools and techniques, some of which had never been used before from a research vessel, it was possible to obtain the first density, neutron porosity, resistivity, and natural gamma-ray logs (Shipboard Scientific Party, 1995b, 1995c). Moore et al. (1995), using bulk density data collected from logging-while-drilling (LWD) to infer fluid pressures in Site 948, showed the existence of excess fluid pressures near fault zones and in the décollement. This was the first clear experimental evidence for the existence of near lithostatic fluid pres-

ures at the base of an accretionary prism, which have been proposed based on theoretical reasoning (Hubbert and Rubey, 1959) or numerical models (Davis et al., 1983).

#### Hole 948C

Building on the results of the highly successful drilling of Site 671 during Leg 110, Site 948 was chosen. By recoring the immediate vicinity of the décollement zone penetrated in Hole 671B, Site 948 (Fig. 2A) was to provide the information necessary for the installation of screened casing in this zone. Hole 948C was cored from 420.8 to 592.0 m below seafloor (mbsf) with 95% recovery. A boundary at 513.9 mbsf separates the lower Miocene and upper Oligocene lower unit (Unit III) consisting of greenish gray claystone from the upper unit (Unit II), which is characterized by gray claystone with nanofossils and variegated claystone with thin interbeds of tuff and altered volcanic ash of undetermined to late Miocene age (Fig. 3A). The décollement (498–529 mbsf) is defined by a succession of zones of scaly fabric, fracture networks or stratal disruption, and structurally intact sediments (Shipboard Scientific Party, 1995b). Whereas the boundary of the décollement zone is gradational at the bottom, it is sharp at the top. The lithologic boundary between Units II and III at 513.9 mbsf also separates the brittle deformation above from a more ductile type of deformation below. Anisotropy of magnetic susceptibility (AMS) data indicate horizontal, east–west shortening in the prism, which changes immediately below the décollement to a geometry consistent with a vertical compaction fabric that also prevails in the underthrust domain.

#### Hole 949B

In the area of Site 949, the décollement was modeled as a low-velocity, high-porosity zone occurring at about 375 mbsf based on its seismic signature (Shipley et al., 1994). The objective of drilling at Site 949 was therefore the comparison of the characteristics of the dé-

<sup>1</sup>Shipley, T.H., Ogawa, Y., Blum, P., and Bahr, J.M. (Eds.), 1997. *Proc. ODP, Sci. Results, 156*: College Station, TX (Ocean Drilling Program).

<sup>2</sup>GEOMAR - Research Center for Marine Geosciences, Wischhofstr. 1-3, D-24148 Kiel, Federal Republic of Germany. wbrueckmann@geomar.de

<sup>3</sup>Geological Survey of Canada Atlantic, Bedford Inst. of Oceanography, Box 1006, Dartmouth, Nova Scotia B2Y 4A2, Canada.

<sup>4</sup>Institute for Rock Magnetism, University of Minnesota, Minneapolis, MN 55455, U.S.A.

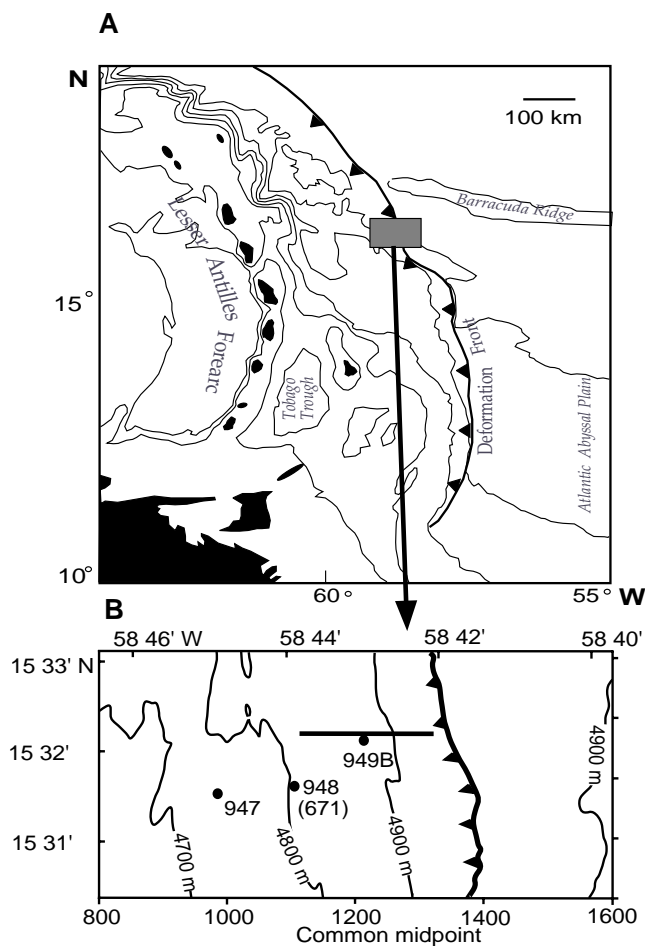


Figure 1. Location map for ODP Leg 156. **A.** Index chart of the Lesser Antilles Island arc. Shaded zone indicates the extent of the Barbados Ridge accretionary prism studied. **B.** Location map showing ODP Legs 156 and 110. Depth contours are based on the evaluation of three-dimensional seismic data (from Shipboard Scientific Party, 1995b).

collement with that of other sites drilled during Leg 156. However, with a core recovery of 39.8% in Hole 949B and 3.5% in Hole 949C, coring at Site 949 was less successful than at Site 948. Although the basic stratigraphy could be established by comparison with other sites cored during DSDP Leg 78A and ODP Leg 110, the limited core recovery precluded any detailed downhole correlation with Site 948. Major thrusts were detected in Cores 156-949B-2X and 13X. The décollement zone is believed to be located between 400 and 437 mbsf; Cores 156-949B-19X and 22X share lithological and deformational characteristics with sediments from this closely defined zone in Hole 948C. The boundary between Units II and III, believed to be responsible for the localization of the décollement, occurs in Core 156-949B-22X (Shipboard Scientific Party, 1995c).

### Acoustic Anisotropy

The term anisotropy refers to the observed quantitative directional dependence of physical properties of sediments. It is well known that most physical property anisotropies result from modifications of the pore-to-particle orientation during deposition and subsequent burial. In normally consolidated sediments with predominantly horizontal bedding  $P$ -wave velocities will increase faster with depth in the direction of the bedding plane than perpendicular to it. The anisotropy

of  $P$ -wave velocity (or acoustic anisotropy) is defined here following Carlson and Christensen (1977) as the difference between velocities in horizontal and vertical direction expressed as percentage of the mean velocity,

$$Ap [\%] = 200 \times (V_{pt} - V_{pl}) / (V_{pt} + V_{pl}), \quad (1)$$

where  $V_{pl}$  is the  $P$ -wave velocity measured in the direction parallel (longitudinal) to the core axis, and  $V_{pt}$  is the  $P$ -wave velocity in the horizontal (transverse) direction. In clay-rich marine sediments, positive transverse anisotropy will vary from 0% near the surface (complete isotropy) to >12% at depths of several hundred meters. In the interpretation of seismic reflection and refraction data, velocity anisotropy has to be taken in consideration because it will determine the mode of wave propagation in the sediment (Bassinot et al., 1993; Carlson and Christensen, 1977; Bachman, 1979; Milholland et al., 1980). Compactional anisotropy, parallel alignment of pores and particles parallel to bedding because of gravitational compaction under increasing overburden, is commonly assumed to be the most important single source for the downhole increase in acoustic anisotropy in fine-grained, clay-rich sediments (Hamilton, 1970; Kim et al., 1983, 1985; O'Brien, 1990).

Another relevant mechanism for the generation of acoustic anisotropy in carbonate-rich marine sediments is the development of preferred orientation of calcite  $c$ -axes normal to bedding (O'Brien, 1990). This will cause anisotropic behavior as the compressional  $P$ -wave velocity is lowest parallel to the  $c$ -axis of calcite crystals, and highest parallel to their  $a$ -axes. Diagenetic reprecipitation of dissolved calcite normal to bedding, due to deformation, is also cited as a possible mechanism to create a uniform orientation of calcite crystals (Carlson and Christensen, 1979; Milholland et al., 1980).

The generation of acoustic anisotropy in the course of deposition in current-dominated environments has been described (Nacci et al., 1974; O'Brien et al., 1980). Comparing compositionally similar argillaceous sediments of hemipelagic and turbiditic origin from the Mississippi Fan, Wetzel (1986, 1987) found clear differences in patterns of inferred strain and acoustic anisotropy. This primary depositional anisotropy is attributed to the preferred orientation of elongated or oblate grains during turbiditic deposition. Other studies have described acoustic anisotropy as an intrinsic sedimentary property induced or amplified by alternating thin layers of isotropic or anisotropic materials (Postma, 1955; Bachman, 1979; Carlson et al., 1983), although this has not been demonstrated to exist under natural conditions. A dependency of acoustic anisotropy in marine sediments on the overall content of  $\text{CaCO}_3$  has also been suspected, although no specific genetic origin is implied. O'Brien (1990) showed, for some calcareous claystones of ODP Holes 603B and 672A, a positive correlation of calcite-content and acoustic anisotropy, whereas an inverse trend was found by Carlson et al. (1983) for pelagic chalks and limestones.

Microstructures have long been acknowledged as an important controlling boundary condition for the development of acoustic anisotropy, but has rarely been quantitatively evaluated. In the exploration industry however, this problem has been extensively studied with the objective of predicting in situ stress orientations in reservoir rocks. Ramos and Rathmell (1989) demonstrated that the orientation of microfractures and microcracks, generated in situ, will control the spatial configuration of acoustic anisotropy in sandstone core samples. By continuously mapping the direction of maximum acoustic anisotropy, they were able to verify the direction of maximum in situ compressive stress, which was also independently determined by other means.

Summarizing, it can be said that acoustic anisotropy has been identified as a very common property of marine sediments, which, although its physical characteristics can be theoretically explained, has

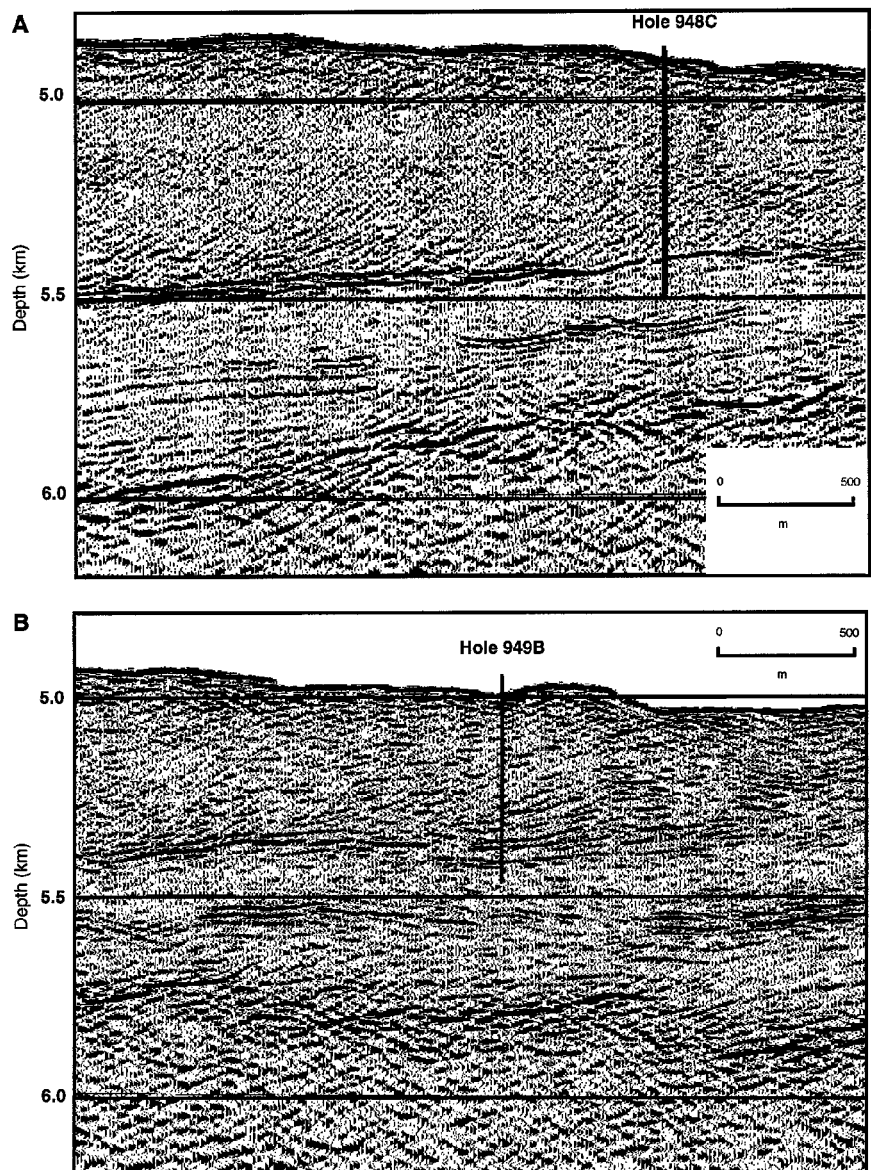


Figure 2. Detail of seismic sections in the (A) Site 948 and (B) Site 949 area illustrating the penetration of Holes 948C and 949B, the position of décollement, accreted sequence, and underthrust sediments (modified from Shipboard Scientific Party, 1995a, 1995b).

yet to be quantitatively determined or constrained through experimental work.

## METHODS

### Shipboard Procedures for the Measurement of *P*-waves

Compressional-wave (*P*-wave) velocity measurements were obtained using two different systems during Leg 156, depending on the degree of lithification of the sediment. *P*-wave velocities were measured in softer sediment using a Digital Sound Velocimeter (DSV) (Shipboard Scientific Party, 1992). Velocity calculation is based on the accurate measurement of the delay time of an impulsive acoustic signal travelling between two pairs of piezoelectric transducers inserted in the split sediment cores parallel and orthogonal to the core axis. The transducers are firmly fixed to a steel plate so that their separation remains constant during the velocity determinations. The longitudinal and transverse transducer separation is 8.5 cm and 4.5 cm, respectively.

The signal used is a 2- $\mu$ s square wave; the transducers have resonances at about 250 and 750 kHz. A dedicated microcomputer con-

trols all functions of the velocimeter. The transmitted and received signals are digitized by a Nicolet 320 digital oscilloscope and transferred to the microcomputer for processing. The DSV software selects the first arrival and calculates sediment velocity.

Periodically, the separation was precisely evaluated by running a calibration procedure in distilled water. A value of sound velocity in distilled water is determined (based on standard equations) for the measured temperature, with the computer calculating the transducer separation using the signal travel time.

The Hamilton Frame Velocimeter was used to measure compressional-wave velocities at 500 kHz in discrete sediment samples when induration made it difficult to insert the DSV transducers into the sediment without making any perturbations around them and in indurated sediments when insertion became impossible. Samples were carefully cut using a double-bladed diamond saw from intact "biscuits." Three measurements were made on each individual sample,  $V_{pl}$  in longitudinal direction, i.e., propagation parallel to the core axis, and  $V_{t1}$  and  $V_{t2}$  in transverse directions, i.e., propagation in a horizontal plane normal to the core axis with a 90° angle between both transverse measurements. To facilitate later reorientation of the transverse velocities using paleomagnetic techniques, a consistent naming con-

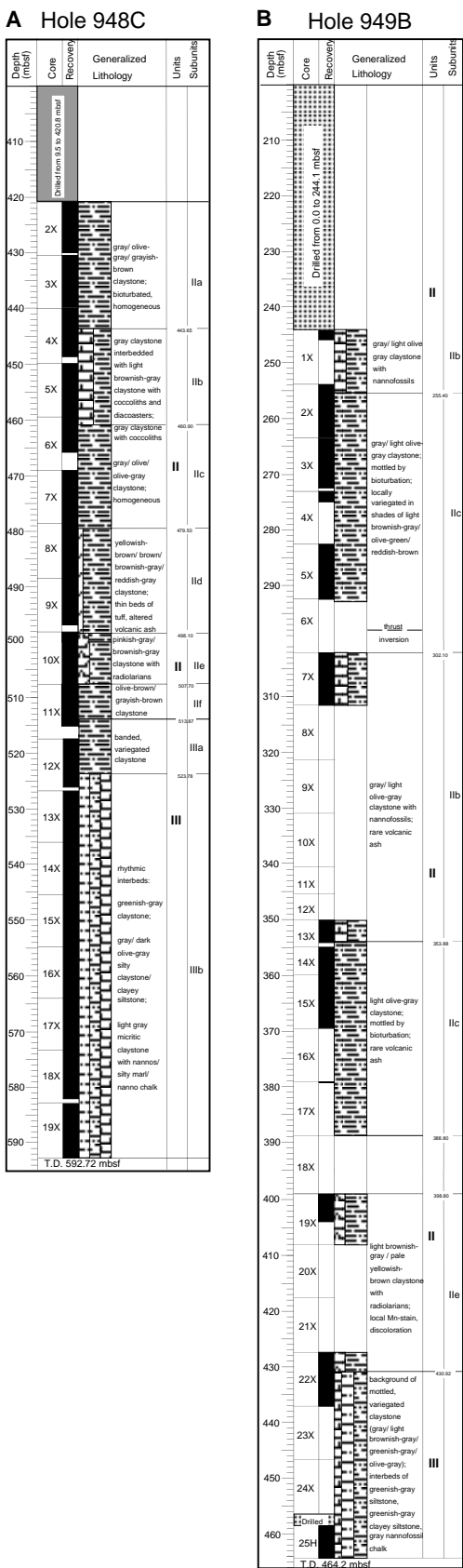


Figure 3. Generalized lithologic section for (A) Hole 948C and (B) Hole 949B. Arrows indicate the position of major thrusts (modified from Shipboard Scientific Party, 1995a, 1995b).

vention was used for  $V_{11}$  and  $V_{12}$  with respect to the surface of the split core. Sample thickness was measured directly from the velocimeter-frame lead screw through a linear resistor output to a digital multimeter. Zero traveltimes for the velocity transducers were estimated by linear regression of traveltime versus distance for a series of aluminum and lucite standards. Filtered seawater was used to improve the acoustic contact between the sample and the transducers. The DSV oscilloscope and processing software were used to digitize waveforms and calculate velocities. Measurements were routinely made by propagating the waveform parallel to the core axis (longitudinal) and parallel to the split core surface (horizontal or transverse). This approach then provides a measure of the acoustic anisotropy within the sediments.

### Reorientation Procedure

Reorientation of the rotated portions of XCB cores was accomplished using paleomagnetic results. Discrete samples were alternately field demagnetized, and the characteristic remanence direction was calculated using principal component analysis. The declinations of the characteristic directions were then rotated to  $360^\circ$  (for normal polarity) or  $180^\circ$  (for reversed polarity). An orientation procedure using paleomagnetic data is described in Taira, Hill, Firth, et al. (1991), and in Byrne et al. (1991). In general, reorientation of structural and magnetic fabric data using paleomagnetic results was highly successful during Leg 156.

### SHIPBOARD RESULTS

#### Compressional-wave (P-wave) Velocity Data, Hole 948C

As is true for all physical properties from Hole 948C, the velocity data are characterized by an apparent lack of correlation with recent physical processes generally thought to be associated with accretionary prism dynamics. Although an offset can be found in all downhole profiles of physical properties across the décollement zone, this change is more likely to be governed by the difference in lithologic composition above and below the décollement than by changes in the in situ stress state or fluid-flow activity within this depth interval (Shipboard Scientific Party, 1995b). The compressional-wave velocities from core samples also display an unusually large degree of variation over most of the core interval in Hole 948C (Fig. 4A). For sediments of lithologic Subunits IIA through IID, no apparent downhole trend in  $P$ -wave velocities is found, with values varying between 1766 and 1608 m/s. The upper part of the décollement zone shows an anomalous decrease in velocity from 1692 to 1581 m/s over a 25-m interval, coinciding with decreasing porosity and an increase in bulk and grain density. The lower part of the décollement zone as well as the lithologic Unit III below it are characterized by velocities scattering over a wide range from 1531 to 1755 m/s. The overall pattern observed in the longitudinal  $P$ -wave velocities can also be found in the transverse velocities. In general, longitudinal and transverse  $P$ -wave velocities show a fair amount of separation from 421 to 495 mbsf, and they are closely matching between 490 and 510 mbsf, whereas they are extremely variable between 508 and 592 mbsf. The offset from higher to lower average  $P$ -wave velocities at 510 mbsf is controlled by a change in the sediment composition between lithologic Subunits IIe and IIe. The high degree of dispersion in  $P$ -wave velocities below the décollement with transverse velocities much higher than the longitudinal velocities follows a pattern typical for normally consolidated sediments.  $P$ -wave velocity anisotropy was calculated using the longitudinal and the average transverse velocity,

$$Ap[\%] = 200 \times ((\{V_{pt1} + V_{pt2}\}/2) - V_{pl}) / ((\{V_{pt1} + V_{pt2}\}/2) + V_{pl}). \quad (2)$$

The varying degree of dispersion between transverse and longitudinal  $P$ -wave velocities in the two domains is clearly imaged in the  $P$ -

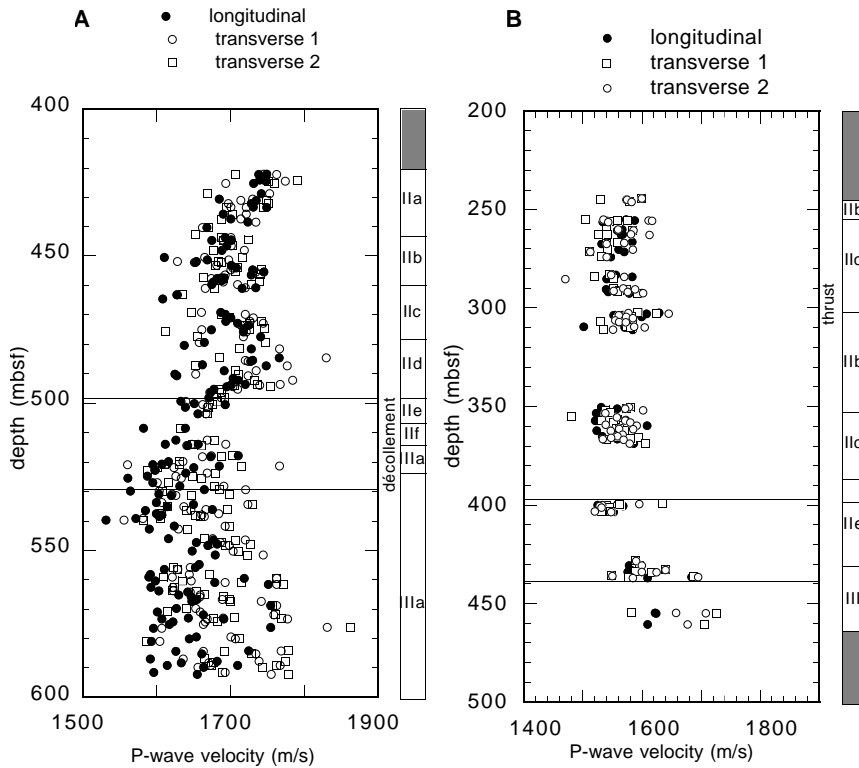


Figure 4. Shipboard *P*-wave velocity data from (A) Holes 948C and (B) Hole 949B, showing measurements longitudinal and transverse (1,2) orientation to the core axis (from Shipboard Scientific Party, 1995a, 1995b).

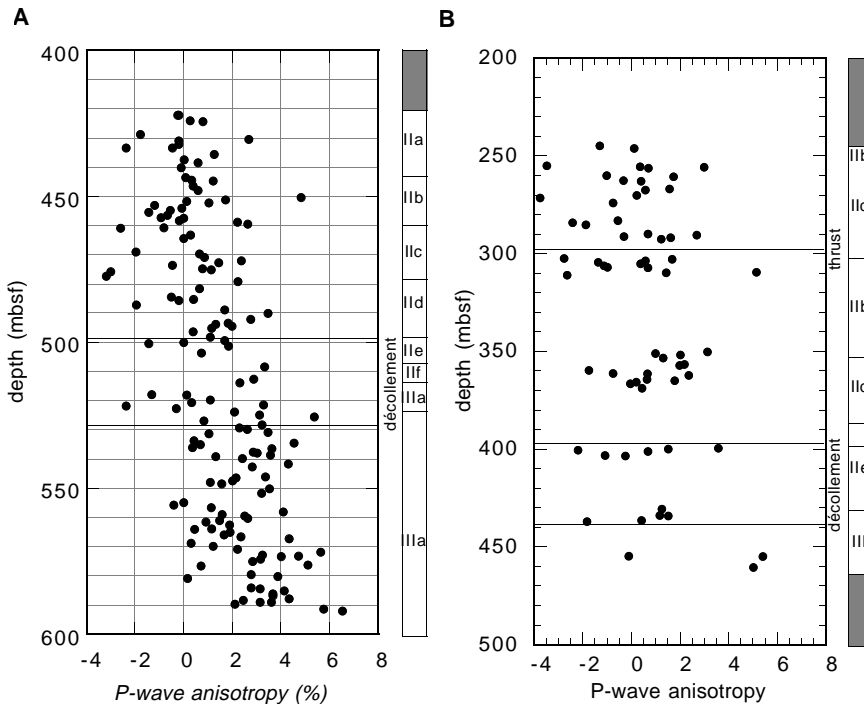


Figure 5. Acoustic anisotropy data from (A) Hole 948C and (B) Hole 949B shipboard data (from Shipboard Scientific Party, 1995a, 1995b).

wave velocity anisotropy. In the accreted section above the décollement, the downhole increase of the *P*-wave velocity anisotropy is very gradual (Fig. 5A), whereas a much stronger increase with depth is apparent in the underthrust sequence.

**Compressional-wave (*P*-wave) Velocity Data, Hole 949B**

Like all other shipboard datasets the velocity data display a discontinuous downhole profile related to the poor recovery in Hole 949B (Fig. 4B). The velocity data set can be divided into three con-

tinuous groups of measurements. The longest coherent downhole record extends from 244 to 311 mbsf (Cores 156-949B-1X through 7X), with velocities ranging from 1532 to 1629 m/s. Despite large scatter, a slight downhole increase in the average velocity is evident.

Between 350 and 369 mbsf (Cores 156-949B-13X through 15X), velocities vary from 1522 m/s in the shallower part to 1608 m/s in the deeper part of the interval, delineating a moderately scattered trend of increasing velocity with depth. The very limited recovery within the presumed décollement zone between 390 and 445 mbsf only allowed a few *P*-wave measurements. Data from Core 156-949B-19X in the

upper part of this zone range from 1525 to 1554 m/s over an interval of only a few meters. Velocities in Cores 156-949B-22X and 23X at the bottom of the décollement zone are significantly higher, ranging from 1576 to 1684 m/s.

Only two reliable  $P$ -wave measurements were obtained in the top of the underthrust sediments (Core 156-949B-25H and Core 156-949C-7R), yielding an average velocity of 1618 m/s, comparable to that determined in Hole 948C.

As in Hole 948C, longitudinal and transverse velocities in the underthrust sediments show a compositionally controlled higher dispersion.

The downhole profile of transverse  $P$ -wave anisotropy displays an equally large degree of scatter without an apparent trend throughout all cored intervals in Hole 949B (Fig. 5B). The scatter is largest in the topmost interval (Cores 156-949B-1X through 7X), with anisotropy ranging from  $-3.76\%$  to  $5.14\%$ . It ranges from  $-1.7\%$  to  $2.3\%$  in Cores 156-949B-13X through 15X, from  $-2.2\%$  to  $3.57\%$  within the décollement zone, and from  $0.1\%$  to  $5.4\%$  in the underthrust section. Again, the discontinuous downhole profile precludes any detailed interpretation of the  $P$ -wave anisotropies.

## RESULTS

Using paleomagnetic techniques, a subset of  $P$ -wave measurements on individual samples from Holes 948C and 949B were reoriented to yield true geographical direction.

A total of 71 measurements of  $V_{t1}$  and  $V_{t2}$  from Hole 948C and 41 measurements from Hole 949B were successfully reoriented. The orientation of  $T_{\min}$ , the slower of the two  $P$ -wave measurements in transverse directions to the core axis,  $V_{pt1}$  and  $V_{pt2}$ , shows a clear correlation with presumed compressive stress. The direction of the maximum in situ stress in the accreted section is assumed to be parallel to the direction of the plate convergence vector (PCV) of  $78^\circ$  (Deng and Sykes, 1995). This assumption is based on AMS orientation data presented in Housen et al. (1996), which are consistent with lateral shortening parallel to the PCV in the prism sediments above the décollement. The bulk of all reoriented  $P$ -wave measurements in the accretionary prism domain in Hole 948C yield a  $T_{\min}$  oriented perpendicular to the convergence vector (Fig. 6A), and a single sample could not be identified where  $T_{\min}$  parallels the subduction vector.

In the underthrust domain, several preferred orientations for  $T_{\min}$  were observed, most prominently one between  $0^\circ$  and  $20^\circ$  and a broad maximum between  $60^\circ$  and  $100^\circ$ , clustered around the PCV at  $78^\circ$  (Fig. 6A). Because of the much smaller number of reoriented  $P$ -wave measurements from Hole 949B, only the accretionary prism domain can be evaluated. As in Hole 948C,  $T_{\min}$  in the accretionary prism domain is predominantly oriented normal to the convergence vector, although an additional strong component can be identified that clusters between  $20^\circ$  and  $60^\circ$  (Fig. 6B). When interpreting the results of the reorientation procedure, it has to be kept in mind that the random orientation of the split core determines the orientation of the sample cube faces cut for  $P$ -wave velocity measurements. For a smaller number of samples, as is the case for Hole 949B, it is conceivable that the true orientation of the maximum  $P$ -wave velocity is not clearly imaged.

For further evaluation of the observed preferential orientation of transverse  $P$ -wave velocities, acoustic anisotropy in Hole 948C above and below the décollement zone was calculated and plotted as a function of true geographical orientation.

To facilitate the further evaluation of directional acoustic properties,  $P$ -wave anisotropy was calculated using  $T_{\max}$ ,

$$Ap [\%] = 200 \times (V_{ptmax} - V_{pt}) / (V_{ptmax} + V_{pt}), \quad (3)$$

where  $V_{ptmax}$  is  $T_{\max}$ , the higher of the two  $P$ -wave velocities measured normal to the core axis. The orientation pattern of acoustic

anisotropy does not show clear maxima in the accretionary prism domain, and no samples were found to have maximum acoustic anisotropy perpendicular to the convergence vector (Fig. 7A). Similarly, no obvious preferred orientation of acoustic anisotropy data is evident in the underthrust domain (Fig. 7B).

## DISCUSSION

It is difficult to evaluate directional dependence of acoustic properties observed in the Barbados accretionary complex without references to other accretionary systems. For the Nankai Trough accretionary prism it has been shown that the compressive tectonic regime will alter the directional properties of physical parameters like  $P$ -wave velocity of sediment (Brückmann et al., 1993). Preferential orientation of  $P$ -wave velocities can be used to determine the fracture direction in areas of pervasive microfracturing to identify the orientation of the maximum in situ stress (Ramos and Rathmell, 1989; Yale and Sprunt, 1989). The orientation of microcracks can be inferred from the direction of maximum and minimum  $P$ -wave velocities, as small scale discontinuities will impede and deflect the propagation of sonic energy, yielding highest  $P$ -wave velocities along strike and lowest perpendicular to strike. In the Nankai Trough, the acoustic anisotropy peaks in two directions, parallel and perpendicular to the maximum compressive strain. This is thought to be controlled by two processes operating at the same time: the formation of vertical microfractures normal to the maximum in situ compressive strain after core recovery (stress relief) and the development of vertical tensile microfractures parallel to the maximum compressive strain. Judging from the observed random orientation of the  $P$ -wave velocity anisotropy in both accreted and underthrust domains of Hole 948C, it is unlikely that similar processes are active here. A structural control through the formation of stress relief features can be ruled out here, because the slower horizontal velocity  $T_{\min}$  in the accretionary prism domain in Hole 948C is perpendicular to the plate convergence vector, the inferred direction of the maximum compressive strain (Housen et al., 1996). Opening of cracks as a stress relief process normal to the direction of the maximum stress would result in slowest  $P$ -wave velocities parallel to the plate convergence vector (Fig. 6A), the opposite of what was observed here. The same is true for the accretionary prism domain in Hole 949B (Fig. 6B).

Inclined bedding is another important parameter to be considered. The occurrence of inclined bedding with respect to the core axis would, depending on the dip angle, significantly affect the relative proportions of  $V_{pt1}$ ,  $V_{pt2}$ , and  $V_{pt}$  when measured on a standard physical property cube sample, because of the rotation of the velocity tensor.

Because of the homogeneous nature of the sediments recovered, only a small number of bedding dips in the accretionary prism domain of Hole 948C could be recorded. In addition, biscuiting and fragmentation of core sections precluded shipboard scientists from using paleomagnetic reorientation procedures on a regular basis, so that only an insignificant number of selected marker horizons (Shipboard Scientific Party, 1995b) could successfully be reoriented. It is therefore difficult to directly correlate the observed preferred orientation of slower horizontal  $P$ -wave velocities ( $T_{\min}$ ) with corrected bedding orientations. However, the Shipboard Scientific Party (1995b) reported paleomagnetically reoriented structural data from cores above the décollement that suggest variable bedding dips towards the northeast and west.

A plot of bedding dips vs. depth in Hole 948C clearly distinguished sediments in the accretionary prism domain from those in the underthrust domain (Fig. 8). In the accreted sediments above the décollement, most bedding dips are moderate to steep, from  $20^\circ$  to  $60^\circ$  (Shipboard Scientific Party, 1995b). In the lower half of the décollement zone, from 514.2 to 520.5 mbsf, bedding dips are variable (Fig. 8), ranging from  $18^\circ$  to  $39^\circ$ . From 521 mbsf to the base of the décol-

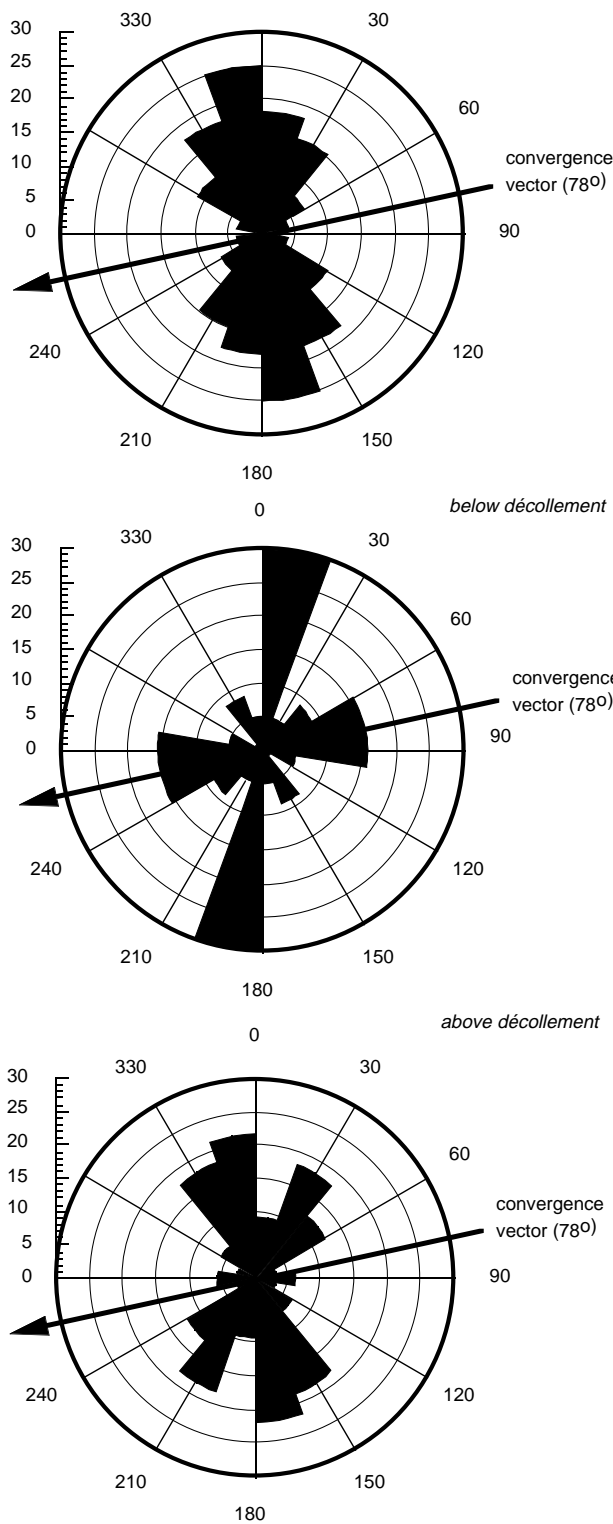


Figure 6. Orientation of lower velocity ( $T_{min}$ ) in individual samples (A) above and below décollement in Hole 948C and (B) above décollement in Hole 949B, presented as a percentage of total counts. Arrow indicates direction of convergence.

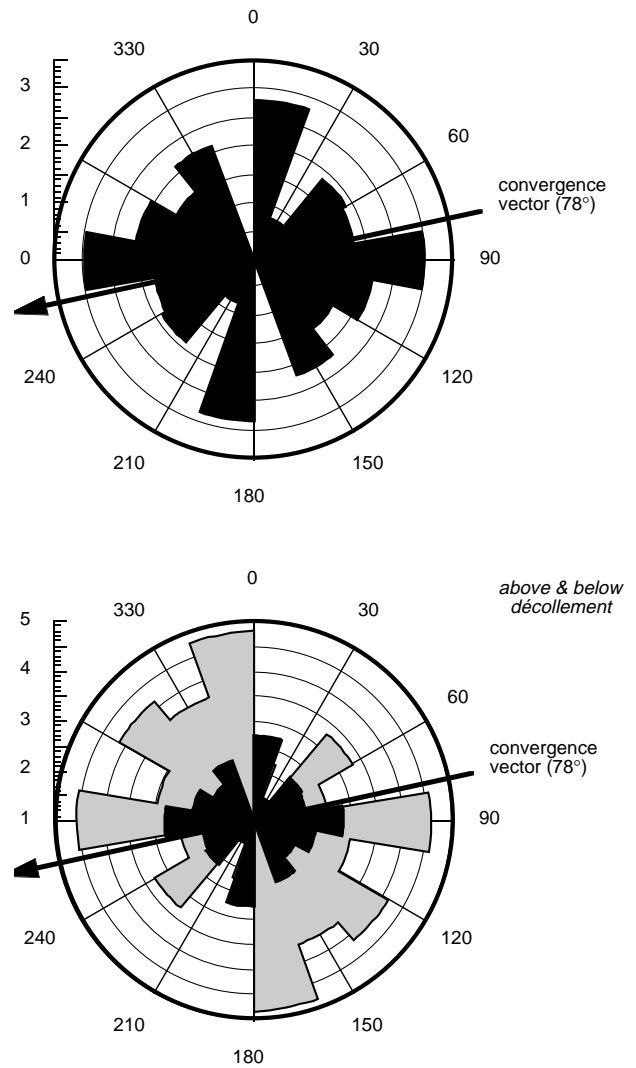


Figure 7. Orientation of transverse velocity anisotropy above and below décollement in (top) Hole 948C and (bottom) Hole 949B averaged over 20° intervals. Arrow indicates direction of convergence.

lement zone, bedding is much more shallowly inclined, identical to the underthrust section where beds are consistently inclined 0°–20°.

Based on this structural information and the limited set of corrected structural data, the observed directional properties of  $P$ -wave velocity in Hole 948C can cautiously be attributed to the variability in bedding inclination. Below the décollement in normally consolidated sediments with predominantly near-horizontal bedding,  $P$ -wave velocities are generally higher in the direction of the bedding plane than perpendicular to it. The smaller difference between longitudinal and transverse  $P$ -wave velocities in samples from the accreted domain is related to generally steeper bedding dips in this part of Hole 948C. When measured in the direction of bedding dip, the transverse  $P$ -wave velocity in the accreted domain will decrease with increasing bedding inclination, whereas the second transverse  $P$ -wave velocity measured normal to it will remain unchanged. This concept is in agreement with the observation of predominantly northwest-oriented  $T_{min}$  values in the accreted domain of Hole 948C. However, in the ab-

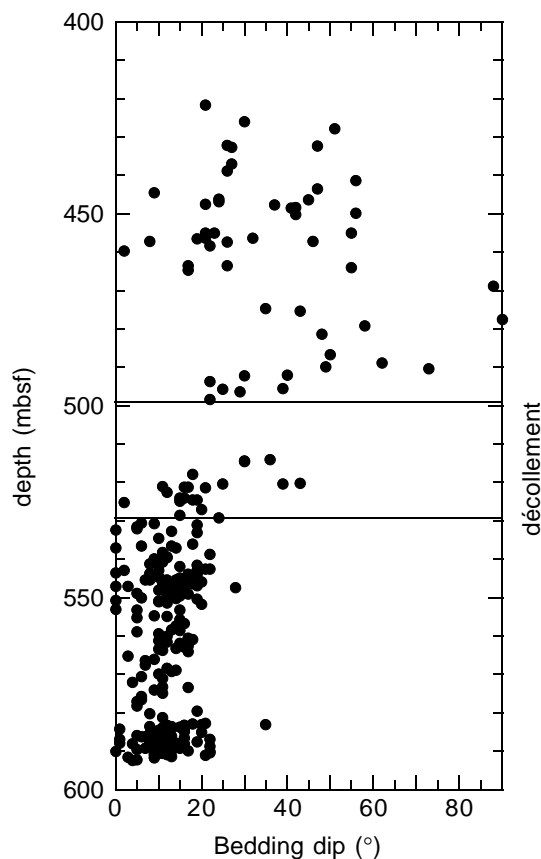


Figure 8. Plot of bedding dip vs. depth in Hole 948C, showing structurally rotated layers above ~521 mbsf and shallow to subhorizontal beds below.

sence of a complete data set of geographically corrected bedding orientations this conclusion can not adequately be tested.

## SUMMARY

To evaluate the possible correlation of preferred orientation of acoustic properties and the direction of maximum compressive strain in the frontal part of the northern Barbados accretionary prism, shipboard  $P$ -wave velocities from Holes 948C and 949B were reoriented to yield  $P$ -wave velocity and  $P$ -wave velocity anisotropy as a function of geographical direction. This information was then used to compare accreted vs. subducted sediments in terms of their directional properties. The bulk of all reoriented  $P$ -wave velocity measurements in the accretionary prism domain in Hole 948C show that the lower of the two transverse velocities ( $T_{\min}$ ) is oriented nearly perpendicular to the convergence vector. In the underthrust domain, several preferred orientations for  $T_{\min}$  were observed, but no strong correlation with the geotectonic reference frame was found. A similar, although less pronounced, pattern was found in the accretionary prism domain in Hole 949B. Unlike the transverse velocity, acoustic anisotropy data does not show a clear pattern in the accretionary prism domain of Hole 948C. In addition, no obvious preferred orientation was identified in the underthrust domain or in the accretionary prism domain of Hole 949B. It is proposed that the observed directional dependence of  $P$ -wave velocity in the accreted sediment domain in Hole 948B is the result of moderate to steeply inclined bedding, although this conclusion can not adequately be tested due to the lack of a true geographic reference for the structural data.

## ACKNOWLEDGMENTS

Financial support for this study was provided by Deutsche Forschungsgemeinschaft through Grant Br 1075-5/1. Extensive reviews provided by J. Morgan and T. Byrne greatly helped revising this manuscript. All this is gratefully acknowledged.

## REFERENCES

- Bachman, R.T., 1979. Acoustic anisotropy in marine sediments and sedimentary rocks. *J. Geophys. Res.*, 84:7661–7663.
- Bassinot, F.C., Marsters, J.C., Mayer, L.A., and Wilkens, R.H., 1993. Variations of porosity in calcareous sediments from the Ontong Java Plateau. In Berger, W.H., Kroenke, L.W., Mayer, L.A., et al., *Proc. ODP, Sci. Results*, 130: College Station, TX (Ocean Drilling Program), 653–661.
- Biju-Duval, B., Moore, J.C., et al., 1984. *Init. Repts. DSDP, 78A*: Washington (U.S. Govt. Printing Office).
- Brown, K.M., Bekins, B., Clennell, B., Dewhurst, D., and Westbrook, G., 1994. Heterogeneous hydrofracture development and accretionary fault dynamics. *Geology*, 22:259–262.
- Byrne, T., Brückmann, W., Owens, W., Lallemand, S. and Maltman, A., 1991. Structural synthesis: correlations of structural fabrics, velocity anisotropy, and magnetic susceptibility data. In Hill, I., Taira, A., Firth, J.V. et al., *Proc. ODP, Sci. Results*, 131: College Station, TX (Ocean Drilling Program), 365–377.
- Brückmann, W., Moran, K., and Taylor, E., 1993. Acoustic anisotropy and microfabric development in accreted sediment from the Nankai Trough. In Hill, I.A., Taira, A., Firth, J.V., et al., *Proc. ODP, Sci. Results*, 131: College Station, TX (Ocean Drilling Program), 221–233.
- Carlson, R.L., and Christensen, N.I., 1977. Velocity anisotropy and physical properties of deep-sea sediments from the western South Atlantic. In Supko, P.R., Perch-Nielsen, K., et al., *Init. Repts. DSDP, 39*: Washington (U.S. Govt. Printing Office), 555–559.
- , 1979. Velocity anisotropy in semi-indurated calcareous deep-sea sediments. *J. Geophys. Res.*, 84:205–211.
- Carlson, R.L., Schaftenaar, C.H., and Moore, R.P., 1983. Causes of compressional-wave anisotropy in calcareous sediments from the Rio Grande Rise. In Barker, P.F., Carlson, R.L., Johnson, D.A., et al., *Init. Repts. DSDP, 72*: Washington (U.S. Govt. Printing Office), 565–576.
- Dahlen, F.A., Suppe, J., and Davis, D.M., 1984. Mechanics of fold and thrust belts and accretionary wedges: cohesive Coulomb theory. *J. Geophys. Res.*, 89:10087–10101.
- Davis, D., Suppe, J., and Dahlen, F.A., 1983. Mechanics of fold-and-thrust belts and accretionary wedges. *J. Geophys. Res.*, 88:1153–1172.
- Deng, J., and Sykes, L.R., 1995. Determination of Euler pole for contemporary relative motion of Caribbean and North American plates using slip vectors of interplate earthquakes. *Tectonics*, 14:39–53.
- Hamilton, E.L., 1970. Sound velocity and related properties of marine sediments, North Pacific. *J. Geophys. Res.*, 75:4423–4446.
- Housen B.A., Tobin, H.J., Labaume, P., Leitch E.C., Maltman, A.J., Shipley, T., Ogawa, Y., Ashi, J., Blum, P., Brückmann, W., Felice, F., Fisher, A., Goldberg, D., Henry, P., Jurado, M.J., Kastner, M., Laier, T., Meyer, A., Moore, J.C., Moore, G., Peacock, S., Rabaute, A., Steiger, T., Underwood, M., Xu, Y., Yin, H., Zheng, Y., and Zwart, G., 1996. Strain decoupling across the décollement of the Barbados accretionary prism. *Geology*, 24: 127–130.
- Hubbert, M.K., and Rubey, W.W., 1959. Role of fluid pressures in mechanics of overthrust faulting, Part 1. Mechanics of fluid-filled porous solids and its application to overthrust faulting. *Geol. Soc. Am. Bull.*, 70:115–166.
- Karig, D.E., and Morgan, J.K., 1994. Tectonic deformation: stress paths and strain histories. In Maltman, A. (Ed.), *The Geological Deformation of Sediments*: London (Chapman and Hall), 167–204.
- Kim, D.-C., Katahara, K.W., Manghnani, M.H., and Schlanger, S.O., 1983. Velocity and attenuation in deep-sea carbonate sediments. *J. Geophys. Res.*, 88:2337–2343.
- Kim, D.-C., Manghnani, M.H., and Schlanger, S.O., 1985. The role of diagenesis in the development of physical properties of deep-sea carbonate sediments. *Mar. Geol.*, 69:69–91.
- Millholland, P., Manghnani, M.H., Schlanger, S.O., and Sutton, G., 1980. Geoacoustic modeling of deep-sea carbonate sediments. *J. Acoust. Soc. Am.*, 68:1351–1360.

- Moore, J.C., Mascle, A., et al., 1990. *Proc. ODP, Sci. Results*, 110: College Station, TX (Ocean Drilling Program).
- Moore, J.C., Mascle, A., Taylor, E., Andreieff, P., Alvarez, F., Barnes, R., Beck, C., Behrmann, J., Blanc, G., Brown, K., Clark, M., Dolan, J.F., Fisher, A., Gieskes, J., Hounslow, M., McLellan, P., Moran, K., Ogawa, Y., Sakai, T., Schoonmaker, J., Vrolijk, P., Wilkens, R.H., and Williams, C., 1988. Tectonics and hydrogeology of the northern Barbados Ridge: results from Ocean Drilling Program Leg 110. *Geol. Soc. Am. Bull.*, 100:1578–1593.
- Moore, J.C., Shipley, T.H., Goldberg, D., Ogawa, Y., Filice, F., Fisher, A., Jurado, M.-J., Moore, G.F., Rabaute, A., Yin, H., Zwart, G., Brückmann, W., Henry, P., Ashi, J., Blum, P., Meyer, A., Housen, B., Kastner, M., Labaume, P., Laier, T., Leitch, E.C., Maltman, A.J., Peacock, S., Steiger, T.H., Tobin, H.J., Underwood, M.B., Xu, Y., Zheng, Y., 1995. Abnormal fluid pressures and fault-zone dilation in the Barbados accretionary prism: evidence from logging while drilling. *Geology*, 23:605–608.
- Nacci, V.A., Wang, M.C. and Gallagher, J., 1974. Influence of anisotropy and soil structure on elastic properties of sediments. In Hampton, L. (Ed.), *Physics of Sound in Marine Sediments*: New York (Plenum), 63–88.
- O'Brien, D.K., 1990. Physical, acoustic, and electrical properties of deep-sea sediments [Ph.D. dissert.]. Univ. Hawaii.
- O'Brien, N.R., Nakazawa, K. and Tokuhashi, S., 1980. Use of clay fabric to distinguish turbiditic and hemipelagic siltstones and silt. *Sedimentology*, 27:47–61.
- Postma, G.W., 1955. Wave propagation in a stratified medium. *Geophysics*, 20:780–806.
- Ramos, G.G. and Rathmell, J.J., 1989. Effects of mechanical anisotropy on core strain measurements for in situ stress determination. In Tomich, J. F.O. (Ed.), *Formation Evaluation and Reservoir Geology*. Exxon Prod. Res., Soc. Pet. Eng. AIME, 64.
- Shipboard Scientific Party, 1992. Explanatory notes. In Mayer, L., Pisias, N., Janecek, T., et al., *Proc. ODP, Init. Repts.*, 138 (Pt. 1): College Station, TX (Ocean Drilling Program), 13–42.
- , 1995a. Introduction. In Shipley, T.H., Ogawa, Y., Blum, P., et al., *ODP, Init. Repts.*, 156: College Station, TX (Ocean Drilling Program), 3–11.
- , 1995b. Site 948. In Shipley, T.H., Ogawa, Y., Blum, P., et al., *ODP, Init. Repts.*, 156: College Station, TX (Ocean Drilling Program), 87–192.
- , 1995c. Site 949. In Shipley, T.H., Ogawa, Y., Blum, P., et al., *ODP, Init. Repts.*, 156: College Station, TX (Ocean Drilling Program), 193–257.
- Shipley, T.H., Moore, G.F., Bangs, N.L., Moore, J.C., and Stoffa, P.L., 1994. Seismically inferred dilatancy distribution, northern Barbados Ridge décollement: implications for fluid migration and fault strength. *Geology*, 22:411–414.
- Taira, A., Hill, I., Firth, J.V., et al., 1991. *Proc. ODP, Init. Repts.*, 131: College Station, TX (Ocean Drilling Program).
- Wetzel, A., 1986. Anisotropy and modes of deposition of pelitic Mississippi Fan deposits. In Bouma, A.H., Coleman, J.M., Meyer, A.W., et al., *Init. Repts. DSDP, 96*: Washington (U.S. Govt. Printing Office), 811–817.
- , 1987. Sedimentological significance of strain and sonic velocity anisotropy in fine-grained turbiditic and hemipelagic deep-sea sediments: an example from the Mississippi Fan. *Mar. Geol.*, 74:191–207.
- Yale, D.P., and Sprunt, E.S., 1989. Prediction of fracture direction using shear acoustic anisotropy. *Log Analyst*, 30:65–70.

**Date of initial receipt: 5 February 1996**

**Date of acceptance: 9 July 1996**

**Ms 156SR-017**